

# Supplementary Material for “Structural organization of large and very-large scales in turbulent pipe flow simulation”

J. R. Baltzer, R. J. Adrian, and X. Wu

## 1 Structure Lengths at $y^+ = 30$

While the main text focused on structure lengths at  $y/R = 0.15$ , the structure lengths are also similarly calculated nearer the wall at  $y^+ = 30$  in figure I. While this position is where the buffer and logarithmic layers meet with relatively strong influence of the near-wall motions, which are not the emphasis of this study, the length distribution is instructive. The histogram uses the same threshold value of  $u' = -0.1U_{\text{bulk}}$  that was used in the main text for  $y/R = 0.15$ , where this value was approximately the magnitude of the local  $u'$  rms value of  $0.0995U_{\text{bulk}}$ . At  $y^+ = 30$ , the local  $u$  rms value is  $0.133U_{\text{bulk}}$ , so the threshold corresponds to a relatively weaker fluctuation when scaled by rms  $u'$  fluctuation, thereby promoting the extraction of longer structures. The results indicate that long motions also exist in this region, consistent with footprints of taller VLSMs extending downward near the wall (Hutchins & Marusic, 2007), which will be further discussed.

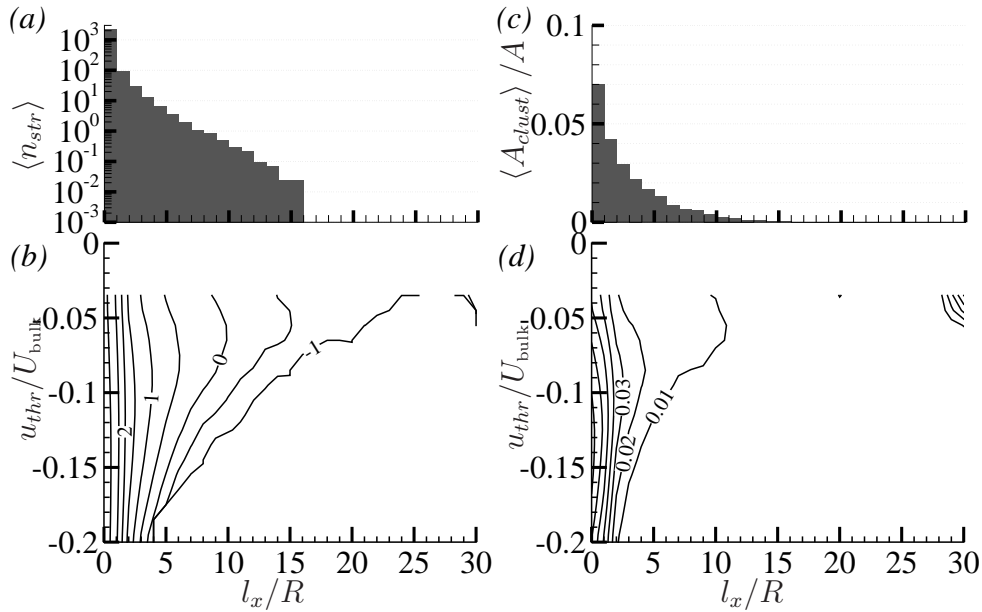


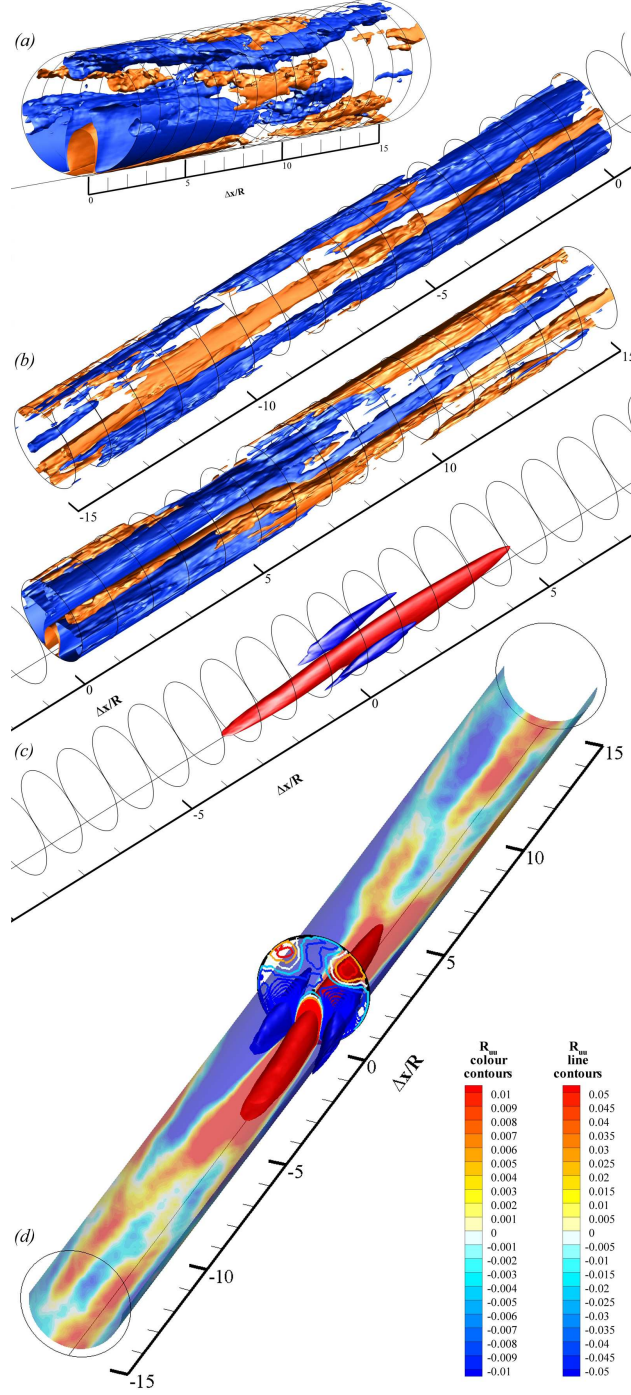
Figure I: Histograms of streamwise length of contiguous regions of negative  $u'$  fluctuation as in figure 3, except  $y^+ = 30$  (a) and (c) correspond to a threshold value of  $u'_{thr}/U_{\text{bulk}} = -0.10$ .

## 2 Three-Dimensional Correlation

The three-dimensional version of the two-point correlation provides additional insight into the mean structure associated with streamwise velocity fluctuations, including the radial aspects of these structures. In this case, a  $y$  reference location (radius) is chosen, but instead of displaying the two-point correlation at the same  $y$  (as in the case of the two-dimensional  $x$ - $\theta$  presentation), the correlation values are shown involving points at all  $y$  locations while the reference  $y$  remains fixed. Figures II and III display isosurfaces of three-dimensional two-point correlation for three representative reference heights of  $y_{\text{ref}}^+ = 30, 101, 250$ . In each visualization, the event or reference position is placed at a position elevated by  $y_{\text{ref}}$  above the wall at the streamwise centre of the pipe. Each two-point correlation is visualized at two sets of positive and negative isosurface values, with the stronger levels in figure II(c) used to display the main character of the motions. The overall form of the motions is that of a long streamwise-elongated region of positive correlation (red) extending down near to the wall and above the event, with two shorter (in part because they are weaker) parallel regions of negative correlation (blue) azimuthally offset. The weaker isosurface value in figure II(a-b) provides a radial perspective of the weaker correlated motions that appear in figure 7 of the main text.

The visualizations in figures II and III show that the streamwise-azimuthal patterns for low threshold values remain consistent over a wide radial extent in each case. Thus, the overall organization follows the interpretation developed for  $x$ - $\theta$  surfaces. The radial coherence is a statistical consequence of the radial extents observed in instantaneous  $u'$  structures (§4). The persistence of these structures down to the wall supports the concept of footprints (Hutchins & Marusic, 2007), particularly with the very long structures that are associated with the low correlation values. At these correlation values, the structures are relatively uniform in radial extent, whereas the structures associated with higher correlation levels have a more ramp-like character, particularly for the positive correlation. The planar  $x$ - $y$  cross-section of this three-dimensional two-point correlation for  $y_{\text{ref}}^+ = 101$  (figure II(d)) with no azimuthal displacement was displayed in figure 6. Figure II(d) also illustrates the relation to the cylindrical surfaces when  $y = y_{\text{ref}}$ , as displayed in figure 7, and to the plane for  $\Delta x = 0$  that is considered in §6. In figure II(d), only the azimuthal half corresponding to  $|\Delta\theta| \leq 90^\circ$  for  $y = y_{\text{ref}}$  is shown to clarify the relationship of this surface with the three-dimensional regions of strongest correlation.

For these visualizations of figures II and III, in which the isosurfaces fill the entire domain of displacements, the domain is split at  $\Delta x = 0$  to reveal spatial arrangements. Both halves are shown, and the split at  $\Delta x = 0$  reveals the behaviour at that plane. As described in §5.4, though the underlying patterns are generally clear but probably affected by the set of included fields for this level of convergence, particularly at large displacement distances, the weaker structures should be understood as indicative of the underlying structure with their precise arrangement possibly sensitive to the set of fields included in the averaging. The included set of reference  $y$  values indicate how the two-point correlation structure changes for three regimes of reference  $y$ , and the cut at  $\Delta x = 0$  displays the behaviour of  $R_{uu}(\Delta\theta, y, y_{\text{ref}})$ . Overall, the patterns at greater distances from the reference point than those associated with the smallest motions that are reflected in the two-point correlation are consistent with VLSMs organized as previously discussed with radial extents on the order of the pipe radius. This behaviour is consistent for reference points near the wall at  $y_{\text{ref}}^+ = 30$  ranging through reference points above the log layer at  $y_{\text{ref}}^+ = 250$  or  $y_{\text{ref}} = 0.36R$ .



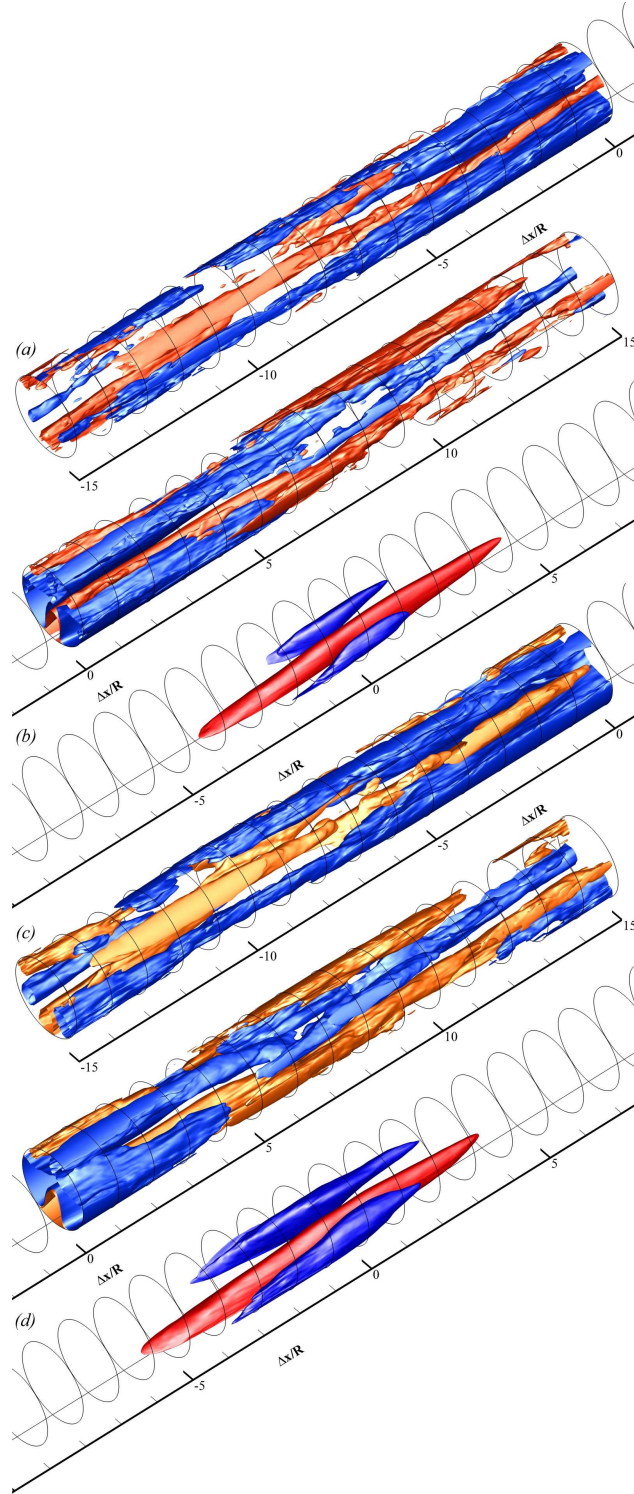


Figure III: Three-dimensional two-point correlation  $R_{uu}$  for reference (event) locations of  $y^+ = 101$  (a,b) and  $y^+ = 250$  (c,d). Correlation coefficient values of isosurfaces are (a,c)  $\pm 0.05$  and (b,d)  $\pm 0.1$ .